IEEE Access
Multidisciplinary ⋮ Rapid Review ⋮ Open Access Journal

Received January 15, 2022, accepted January 29, 2022, date of publication January 31, 2022, date of current version February 8, 2022.

Digital Object Identifier 10.1109/ACCESS.2022.3148316

Security-Constrained Unit Commitment for Hybrid VSC-MTDC/AC Power Systems With High Penetration of Wind Generation

ZHUOYU JIANG[1], YI LIU[2], ZHE KANG[1], TAO HAN[1], AND JING ZHOU[1]
[1]Three Gorges Power Corporation Ltd., Yichang 443000, China
[2]Beijing Ling Yang Wei Ye Technology Company Ltd., Beijing 100176, China

Corresponding author: Yi Liu (1159170349@qq.com)

This work was supported by the research project of China Three Gorges Corporation under Grant 202103521.

ABSTRACT This paper presents the solution to the security-constrained unit commitment (SCUC) problem for hybrid voltage source converter (VSC) based multi-terminal DC/AC (VSC-MTDC/AC) power systems with high penetration of wind generation. The formulated SCUC model presents a detailed representation of the VSCs with two different VSC control strategies considered, constant DC voltage control (master-slave control) and DC voltage droop control. In addition, Grid Code for wind farm connection is considered. Benders decomposition is used to solve the formulated SCUC problem by decomposing it into a master problem for solving unit commitment (UC) and hourly transmission security check subproblems. The final SCUC solution provides an economic and secure operation and control strategy for the meshed MTDC/AC system. Numerical tests illustrated the efficiency of the proposed SCUC model.

INDEX TERMS Wind power, security-constrained unit commitment (SCUC), multi-terminal HVDC (MTDC), AC/DC system, voltage source converter (VSC), Benders decomposition.

I. INTRODUCTION

With the growing concerns about climate change, emissions and environmental issues of competing energy sources, many countries have made great progress in the development of renewable sources of energy, including wind power, in order to meet part of electricity power demand [1]. However, most of the countries in different parts of the world will face significant challenges to transfer large-scale wind power, because the areas with plenty of wind resources are normally far away from load centers. Voltage source converter (VSC) based HVDC is one of the feasible solutions for delivering large-scale remote wind power due to its advantages over both traditional AC system and current source converter (CSC) HVDC [2]. The control flexibility of the VSCs is perfectly suited for constructing a multi-terminal HVDC (MTDC) system thus providing a more rational and efficient solution for the interconnection of wind farms positioning at different locations [3]. In the recent Desertec project [4], European Offshore Supergrid [5] and China Nan'ao MTDC project [6], VSC-MTDC systems are deployed as the backbone receiving and supplying wind generation as well as supporting the existing AC transmission systems.

An earlier work modelled the hybrid AC/DC systems in the unit commitment (UC) problem to analyze the impact of HVDC transmission systems on the economic operation of AC transmission systems, without considering the security constraints [7]. A bibliographical survey of UC problem is presented in [8]. A convenient way to consider AC/DC systems in the security-constrained unit commitment (SCUC) problem is to treat DC terminals as constant power injections in AC transmission system [9]–[11]. This, however, has not considered the dependency of the AC power flow on DC transmission variables. Authors of [12] presents a SCUC model for current source converter (CSC) based AC/DC system. Compared with the current source converter based on high voltage direct current (CSC-HVDC) transmission system, VSC-HVDC can control the active power and reactive power independently and meeting the request of power supply to passive networks. Previous publications of [13], [14] present a mixed-integer second order cone programming (MISOCP) for the hybrid AC-DC power systems. However, the impacts of different control modes of VSC-MTDC have not been included in the study.

The associate editor coordinating the review of this manuscript and approving it for publication was Ton Duc Do.

VSC-MTDC systems' control strategies, such as master control [15] and DC voltage drop control [16], are highly flexible. In both control modes, setting of the corresponding control parameters may change the power flow not only in the DC network, but also the connected AC system, thus impacting the scheduling cost of the entire DC/AC system in terms of the SCUC. FIGURE 1 presents a depiction of operating process for a VSC-MTDC/AC system with wind farms. At first, the dispatch center does the SCUC based on the supply/demand bids and transmission data provided by transmission companies (TRANSCOs). Then the dispatch center will send hourly schedules to the AC system and control strategies to wind farm companies and TRANSCOs.

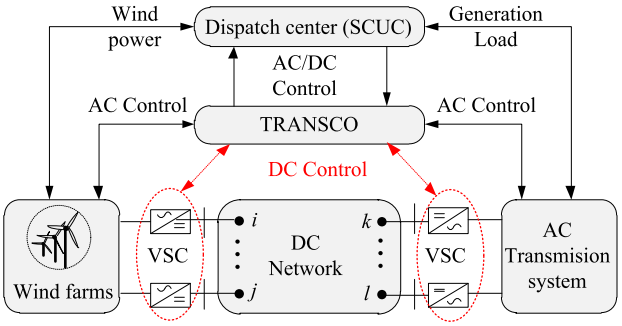

FIGURE 1. Operating process of VSC-MTDC/AC systems with wind farms.

To the best knowledge of the authors, no study has yet addressed the SCUC problem for the meshed VSC-MTDC/AC systems with grid-connected wind generation. To fill the gap, this paper proposes a comprehensive model of security-constrained UC for the VSC-MTDC/AC system with high penetration of wind generation being considered. A method to find the optimal UC solution is presented. The rest of the paper is organized as follows. Section II gives a brief description of the VSC-MTDC system operation model. The SCUC formulation for DC/AC system with grid-connected wind generation and the solution based on Benders decomposition are presented in Section III. with a test case study of the IEEE 14-bus power system is given in Section IV. Section V is the conclusions of the paper.

II. VSC-MTDC SYSTEM MODEL

A. VOLTAGE SOURCE CONVERTER MODEL

FIGURE. 2 shows a typical VSC-DC system connected to an AC bus through a transformer. The AC filter is installed on the AC side of DC terminal, in order to eliminate harmonics generated by the DC system.

A converter, either a rectifier or an inverter, can be modeled as [17]:

$$\begin{aligned} P_{si} &= -U_{si}^2 G_{ti} + U_{si}U_{fi}\left[G_{ti}\cos\left(\delta_{si}-\delta_{fi}\right)\right. \\ &\quad \left. + B_{ti}\sin\left(\delta_{si}-\delta_{fi}\right)\right] \\ Q_{si} &= U_{si}^2 B_{ti} + U_{si}U_{fi}\left[G_{ti}\sin\left(\delta_{si}-\delta_{fi}\right)\right. \\ &\quad \left. + B_{ti}\cos\left(\delta_{si}-\delta_{fi}\right)\right] \end{aligned} \tag{1}$$

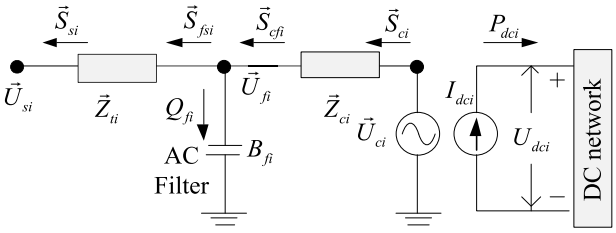

FIGURE 2. Schematic diagram of a VSC-DC system.

$$\begin{aligned} P_{ci} &= U_{ci}^2 G_{ci} - U_{ci}U_{fi}\left[G_{ci}\cos\left(\delta_{fi}-\delta_{ci}\right)\right. \\ &\quad \left. - B_{ci}\sin\left(\delta_{fi}-\delta_{ci}\right)\right] \\ Q_{ci} &= -U_{ci}^2 B_{ci} + U_{ci}U_{fi}\left[G_{ci}\cos\left(\delta_{fi}-\delta_{ci}\right)\right. \\ &\quad \left. + B_{ci}\cos\left(\delta_{fi}-\delta_{ci}\right)\right] \end{aligned} \tag{2}$$

$$\begin{aligned} P_{fsi} &= U_{fi}^2 G_{ti} - U_{fi}U_{si}\left[G_{ti}\cos\left(\delta_{si}-\delta_{fi}\right)\right. \\ &\quad \left. - B_{ti}\sin\left(\delta_{si}-\delta_{fi}\right)\right] \\ Q_{fsi} &= -U_{fi}^2 B_{ti} + U_{fi}U_{si}\left[G_{ti}\sin\left(\delta_{si}-\delta_{fi}\right)\right. \\ &\quad \left. + B_{ti}\cos\left(\delta_{si}-\delta_{fi}\right)\right] \end{aligned} \tag{3}$$

$$\begin{aligned} P_{cfi} &= -U_{fi}^2 G_{ci} + U_{fi}U_{ci}\left[G_{ci}\cos\left(\delta_{fi}-\delta_{ci}\right)\right. \\ &\quad \left. + B_{ci}\sin\left(\delta_{fi}-\delta_{ci}\right)\right] \\ Q_{cfi} &= U_{fi}^2 B_{ci} + U_{fi}U_{ci}\left[G_{ci}\sin\left(\delta_{fi}-\delta_{ci}\right)\right. \\ &\quad \left. - B_{ci}\cos\left(\delta_{fi}-\delta_{ci}\right)\right] \end{aligned} \tag{4}$$

where $G_{ti}+jB_{ti}=1/Z_{ti}$ is the admittance of the converter buses, $G_{ci}+jB_{ci}=1/Z_{ci}$ is the admittance of phase reactors.

Reactive power of lossless AC filter is expressed by

$$Q_{fi} = -U_{fi}^2 B_{fi} \tag{5}$$

Since the AC filter could be eliminated if the modular multilevel converter (MMC) is used [18], in this paper the transformer and the phase reactor will be lumped together, thus to simplify the equations above.

The converter losses are taken into consideration in the model by a generalized equation [17] as follows:

$$P_{lossi} = a_i + b_i \cdot I_{ci} + c_i \cdot I_{ci}^2 \tag{6}$$

where $I_{ci}=\sqrt{P_{ci}^2+Q_{ci}^2}/U_{ci}$ is for per unit system.

The active/reactive power flow balance at the AC filter bus should be satisfied as

$$P_{cfi} - P_{fsi} = 0 \quad \forall i \in \mathbf{N_{DC}} \tag{7}$$

$$Q_{cfi} - Q_{fsi} - Q_{fi} = 0 \quad \forall i \in \mathbf{N_{DC}} \tag{8}$$

B. CONTROL MODES OF THE MTDC TRANSMISSION SYSTEM

1) MASTER-SLAVE CONTROL MODE

By using the master-slave control mode, one converter controls the DC bus voltage around a constant value and the other VSCs operate at constant power control mode.

2) DC VOLTAGE DROOP CONTROL

In this mode, the VSCs work independently to contribute to the balance of total power together with the slack bus. The *i*th VSC controls the DC voltage around a set value. By adjusting the DC current with the slope of R_i to balance the DC power at the same time. One possible case for this control mode is presented in FIGURE. 3. [19] is a good reference for more details for this control strategy.

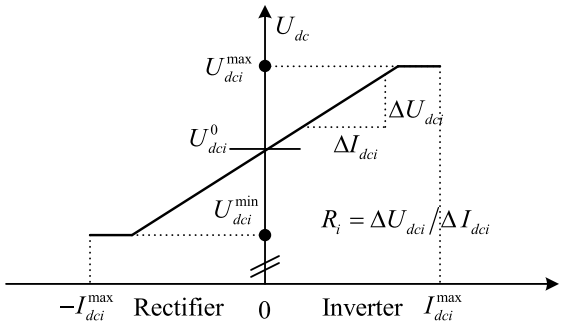

FIGURE 3. DC voltage droop control characteristic.

C. POWER EQUATIONS OF THE VSC-MTDC TRANSMISSION SYSTEM

The active power balance equation of the converter can be formulated as

$$P_{lossi} + P_{ci} + P_{dci} = 0 \tag{9}$$

where P_{dci} and P_{ci} is the active power injected by the converter into the DC and AC side, respectively. P_{dci} can be written as

$$P_{dci} = U_{dci} I_{dci} \quad \forall i \in \mathbf{N_{DC}} \tag{10}$$

where U_{dci} and I_{dci} is the voltage and DC network bus current injection, respectively. The relationship of U_{dci} and I_{dci} can be expressed by

$$I_{dci} = \sum_{j=1}^{n_{DC}} Y_{dcij} \left(U_{dci} - U_{dcj} \right) \quad \forall i \in \mathbf{N_{DC}} \tag{11}$$

where Y_{dcij} is the element of bus admittance matrix $\mathbf{Y_{DC}}$ of the DC network.

D. OPERATION CONSTRAINTS OF THE VSC-MTDC SYSTEM [14]

The following constraints are formulated to ensure the steady state operating point of the converter to satisfy the corresponding PQ capacity limit [20], thus to keep the safe operation of the VSC-MTDC. Equation (12) is the constraint of the IGBT transistor current, Equation (13) is the DC cable current limit, Equation (14) is the constraint of the DC voltage level.

$$-I_{ci\max} \le I_{ci} \le I_{ci\max} \tag{12}$$

$$-I_{dc\max} \le I_{dcij} \le I_{dc\max} \tag{13}$$

$$U_{dci\min} \le U_{dci} \le U_{dci\max} \tag{14}$$

where $I_{ci\max}$ is the maximum converter current limit, I_{dcij} is the current flow of the DC bus, $I_{dc\max}$ is the current rating of the DC cable, $U_{dci\min}/U_{dci\max}$ is the minimum/maximal limit of the DC voltage respectively.

E. GRID CODE FOR WIND FARM CONNECTION

Grid|Code for wind farm connection needs to be considered in the formation of the UC problem. In this paper, the Grid Code in the UK is applied. Requested by the Grid Code, a wind farm should control the reactive power at the connect point. A reactive power capacity of 0.95 power factor lagging to 0.95 leading should be available at the connection point. Hence, such requirements can be represented by the following constraints:

$$Q_{scapi} \ge \alpha P_{si} \tag{15}$$

$$U_{si\min} \le U_{si} \le U_{si\max} \tag{16}$$

where $Q_{scapi} = \sqrt{S_{si}^2 - P_{si}^2}$ is the reactive capacity ruled by the Grid Code, $\alpha = 0.3287$ is the coefficient corresponds to the power factor 0.95, S_{si} is the MVA rating of the *i*th converter, U_{si} is the AC voltage magnitude of the *i*th converter, $U_{si\min} = 0.94$, $U_{si\max} = 1.06$.

III. SCUC FOR VSC-MTDC/AC SYSTEM WITH WIND POWER

A. FORMULATION OF THE SCUC WITH VARIOUS CONSTRAINTS

The SCUC is generalized in Equation (17) where $f(\mathbf{x})$ consists of production cost, starting up and shutting down costs of individual generation unit for the study horizon [21]:

$$\begin{aligned} &\text{Min } f(\mathbf{x}) \\ &\text{S.t. } \mathrm{g1}(\mathbf{x}) \le \mathbf{b1} \\ &\quad \mathrm{ge1}(\mathbf{x}) = \mathbf{be1} \end{aligned} \tag{17}$$

where the vector $\mathbf{x}$ represents the optimization variables, which are composed of on/off status of generation units, startup and shutdown indicators and AC/DC transmission system control variables. The sets of inequality constraints $\mathrm{g1}(\mathbf{x}) \le \mathbf{b1}$ and equality constraints $\mathrm{ge1}(\mathbf{x}) = \mathbf{be1}$ represents the UC constraints such as:

(1) Power balance of the entire VSC-MTDC/AC system.
(2) VSC-MTDC/AC power flow equations with wind power being considered.
(3) Ramping up/down limits of the generations in the AC grid.
(4) Minimum on/off time limits of the generations of the AC grid.
(5) Capacity limits of the generating units in in the grid.

(6) VSC-MTDC/AC network security constraints including the AC/DC transmission flow and bus voltage limits, as well as the limits to the IGBT transistors, converter current, voltage and power of the VSCs, as well as the Grid Code for wind farm connection.
(7) The upper and lower bounds of the MTDC optimization variables composed of linear inequality constraints.
(8) Wind power constraints by considering wind power curtailment:

$$0 \leq P_{\text{wind},t} \leq P_{\text{wind},t}^{\text{mean}} \tag{18}$$

where $P_{\text{wind},t}$ and $P_{\text{wind},t}^{\text{mean}}$ is the expected value and the accommodated wind power, respectively.
(9) Constraints of system reserve requirements (RR) for handling uncertainties in the UC problem. The method of sizing the RR is described in the following subsection.
(10) Time limited corrective controls, such as permissible real power adjustments, for handling contingencies.

B. SPINNING RESERVE REQUIREMENTS FOR HANDLING UNCERTAINTIES IN THE UC PROBLE

Scenario-based stochastic programming and the RR are two of the most common methods to handle uncertainties in the UC problem. Since the former approach needs many scenarios to represent the stochastic nature of uncertainties, the RR approach is adopted in this paper to handle the randomness of wind generation.

Compared with the deterministic criteria, stochastic criteria based on the probabilistic confidence level to meet the forecasted net demand is more flexible and economic. In order to represent the stochastic constraints, the chance-constrained stochastic formulation of the spinning RR is given by Equation (19). The deterministic equivalent of Equation (19) can be formulated as Equation (20):

$$\text{Pro}\left(\sum_{i=1}^{N} u_{it} P_i^{\max} \geq ND_t^f\right) = 1 - \alpha_\lambda \tag{19}$$

$$\sum_{i=1}^{N} u_{it} P_i^{\max} \geq ND_t^{\text{mean}} + \lambda \sigma_{ND,t} \tag{20}$$

where $P_i^{\max}$ is the upper boundary of power output of unit i, $1 - \alpha_\lambda$ is the associated confidence level, u_{it} is a binary variable for the committed status of unit i, ND_t^{mean} is the mean value of net load and ND_t^f is the forecasted net demand, respectively. Here $\lambda = 3$, which means 99.74% of variations are covered [22]. ND_t^{mean} can be calculated based on the expected hourly wind power $P_{\text{wind},t}^{\text{mean}}$ and load demand PD_t^{mean} as follows:

$$ND_t^{\text{mean}} = PD_t^{\text{mean}} - P_{\text{wind},t}^{\text{mean}} \tag{21}$$

The standard deviation of the forecast error of net load, $\sigma_{ND,t}$ can be calculated by the following equation:

$$\sigma_{ND,t} = \sqrt{\sigma_{PD,t}^2 + \sigma_{\text{wind},t}^2} \tag{22}$$

where $\sigma_{PD,t}$ is the standard deviation of load forecast errors which are normally distributed random variables, $\sigma_{\text{wind},t}$ is the standard deviation of wind power forecast errors.

Normally, $\sigma_{PD,t}$ is considered as a percentage of the expected power load demand [23], taken to be 2% in this paper. Wind power forecast errors are also considered to be normally distributed random variables. $\sigma_{\text{wind},t}$ depends heavily on the forecasting horizon and the expected wind power value. For a 24-h forecasting horizon, it can be represented by the following equation [24]:

$$\sigma_{\text{wind},t} = (\alpha \cdot \frac{P_{\text{wind},t}^{\text{mean}}}{P_{installed}} + \beta)\sigma_{w,t} \tag{23}$$

where the standard deviation of normalised wind power forecast error is expressed as a function of forecast horizon, $\sigma_{w,t}$, and the coefficients α and β are borrowed from [24].

C. SOLUTION OF THE SCUC FOR THE VSC-MTDC/AC SYSTEM

The Benders decomposition is applied to solve the SCUC for the VSC-MTDC/AC transmission systems as depicted in FIGURE. 4. The master problem, the UC, is modeled as a linear mixed integer problem (MIP) in the GAMS environment [25], and the CPLEX solver is used to solve the MIP. The solution provides the status and the dispatching active power of each generation unit, as well as the accommodated wind power. The SCUC sub-problem considers mismatches of inequality constraints except the power balance constraint formulated in the master problem. The sub-problem is developed from [26] and it is solved based on the Primal-Dural Interior Point (PDIP) algorithm by adding constraints of the MTDC system to the available open source Matlab toolbox, Matpower [27]. The sub-problem generates Benders cuts or updates the power losses of the whole system for the next UC iteration if the mismatch exists. The interactive procedure will not stop until all mismatches are removed.

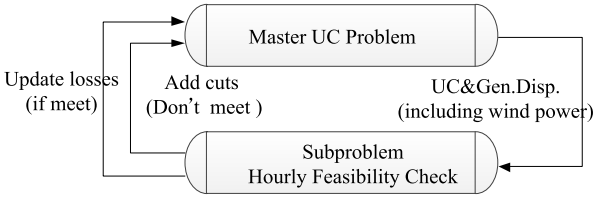

FIGURE 4. SCUC with VSC-MTDC/AC systems.

D. THE SCUC SUB-PROBLEM

The objective function of the sub-problem is:

$$\text{Min } w = \sum_{b=1}^{NB} (\mathbf{MP1}_b + \mathbf{MP2}_b + \mathbf{MQ1}_b + \mathbf{MQ2}_b) \tag{24}$$

where NB is the number of AC buses, $\mathbf{MP_{1b}}, \mathbf{MP_{2b}}$ and $\mathbf{MQ_{1b}}, \mathbf{MQ_{2b}}$ are slack variables vectors of mismatched active power and reactive power at bus b respectively in the

equality constraint:

$$\begin{bmatrix} \mathbf{A}\cdot\mathbf{\Delta P} \\ \mathbf{A}\cdot\mathbf{\Delta Q} \\ \mathbf{0} \end{bmatrix} = [\mathbf{J}]\,\mathbf{X}_t + \begin{bmatrix} \mathbf{P1} \\ \mathbf{Q1} \\ \mathbf{0} \end{bmatrix} - \begin{bmatrix} \mathbf{P2} \\ \mathbf{Q2} \\ \mathbf{0} \end{bmatrix} = \begin{bmatrix} d\mathbf{P_0} \\ d\mathbf{Q_0} \\ d\mathbf{K}_0 \end{bmatrix} \quad (25)$$

where $\mathbf{\Delta P}$ and $\mathbf{\Delta Q}$ is the incremental active/reactive vectors, $d\mathbf{P_0}$ and $d\mathbf{Q_0}$ the initial AC bus active/reactive mismatch vectors, $d\mathbf{K}_0$ the mismatch vector of other equations of the DC/AC system, respectively, $\mathbf{A}$ is the bus-unit incidence matrix, $\mathbf{J}$ the Jacobian matrix, which is given in Appendix A. The vector of decision variables at a certain operating point t for the sub-problem is

$$\mathbf{X}_t^{\mathbf{T}} = [\boldsymbol{\theta}, \mathbf{U}, \mathbf{P_G}, \mathbf{Q_G}, \boldsymbol{\theta_f}, \boldsymbol{\theta_c}, \mathbf{U_f}, \mathbf{U_c}, \mathbf{U_{dc}}, \mathbf{U_{dc}^{Ref}}, \mathbf{P_s^{Ref}}, \mathbf{Q_s^{Ref}}, \mathbf{U_s^{Ref}}] \quad (26)$$

$$\mathbf{X}_t^{\mathbf{T}} = [\boldsymbol{\theta}, \mathbf{U}, \mathbf{P_G}, \mathbf{Q_G}, \boldsymbol{\theta_f}, \boldsymbol{\theta_c}, \mathbf{U_f}, \mathbf{U_c}, \mathbf{U_{dc}}, \mathbf{Q_s^{Ref}}, \mathbf{U_s^{Ref}}, \mathbf{R}] \quad (27)$$

where

$\boldsymbol{\theta}$	Bus voltage angel state variable vector
$\mathbf{U}$	Bus voltage magnitudes state variable vector
$\mathbf{P_G}$	Active power generation control vector
$\mathbf{Q_G}$	Reactive power generation control vector
$\mathbf{U_f}$	Filter bus voltage magnitude state variable vector
$\mathbf{U_c}$	Converter bus voltage magnitude state variable vector
$\boldsymbol{\theta_f}$	Filter bus voltage angle state variable vector
$\boldsymbol{\theta_c}$	Converter bus voltage angle state vector
$\mathbf{U_{dc}}$	Bus voltage state variable vector
$\mathbf{Q_s^{Ref}}$	Scheduled reactive power reference control vector vector
$\mathbf{U_s^{Ref}}$	Scheduled AC bus voltage reference control vector

Note that Equation (26) is for the VSC-MTDC system by applying master-slave control mode with $\mathbf{U_{dc}^{Ref}}$ and $\mathbf{P_s^{Ref}}$ being the scheduled DC bus voltage control vector and active power reference control vector of the converters respectively. Equation (27) is for the DC voltage droop control mode with $\mathbf{R}$ being the slope control vector. In the sub-problem, all generating units except those at the slack bus should satisfy Equation (28):

$$\mathbf{\Delta P} = \mathbf{0}\,\pi \quad (28)$$

If the positive w equals to 0, power losses provided by the sub-problem solution are updated for the master problem. Otherwise, a mismatch Benders cut will be added to the master problem for the next iterative solution:

$$w + \pi\left(\mathbf{P_G} - \hat{\mathbf{P}}_\mathbf{G}\right) + \psi_{up}\mathbf{Q}_{\max}\left(\mathbf{u} - \hat{\mathbf{u}}\right) + \psi_{dn}\mathbf{Q}_{\max}\left(\mathbf{u} - \hat{\mathbf{u}}\right) \le 0 \quad (29)$$

where $\boldsymbol{\pi}$, ψ_{up}, ψ_{dn} are the Lagrange multiplier vectors for constraints (28) and (30), $\mathbf{u}$ is the binary variable vector of the generation status (where 1 indicates the generation unit is committed), $\hat{\mathbf{P}}_\mathbf{G}$ and $\hat{\mathbf{u}}$ are the optimization results in the current iteration, $\mathbf{\Delta Q}_{\min}$ and $\mathbf{\Delta Q}_{\max}$ are the lower and upper limit vectors for incremental unit reactive power, respectively.

$$\mathbf{\Delta Q}_{\min} \le \mathbf{\Delta Q} \le \mathbf{\Delta Q}_{\max} \quad \psi_{up}, \psi_{dn} \quad (30)$$

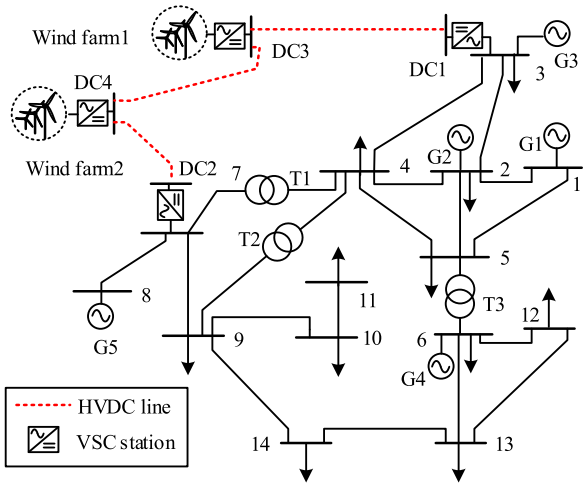

FIGURE 5. Modified IEEE 14-bus system with VSC-MTDC connected wind farms.

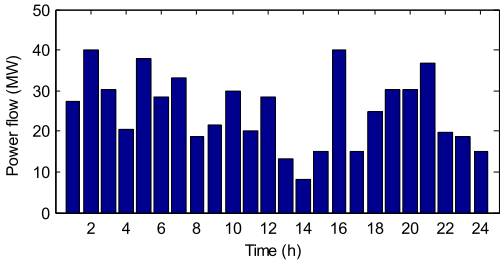

FIGURE 6. Power flow between DC bus 3 and 4.

IV. CASE STUDY

FIGURE.5 shows the modified IEEE 14-bus power system. Two wind farms with a capacity of 70 MW/each are connected to bus 3 and bus 7 through a four-terminal HVDC network. Bus 1 is selected as the slack bus for the AC network. Parameters of this hybrid VSC-MTDC/AC system are given in Appendix B. Two wind power profiles considered in this study are provided in Appendix C. Spinning RR are calculated by using the methods presented in Section III B.

A. MASTER CONTROL MODE

The following cases are studied when the MTDC system adopts the master control mode:

Case1: Based on the method proposed in [12], the SCUC of the AC system without the grid-interconnected wind generation is carried out. This is the base case for the comparison with the SCUC proposed in this paper.

Case2: The SCUC for the meshed VSC-MTDC/AC system is carried out by use of the proposed method in this paper without the limits of the DC-side variables i.e., the lower and upper limits, being imposed. But both maximum and minimum power flow limits of the DC

lines connecting DC bus 3 and 4 are taken to be 0 and the hourly forecasted wind power is assumed to be 0. This case is used to compare with Case1, to verify the correctness of the model proposed.

Case3: The SCUC is carried out by the method proposed in this paper. Various control references for the MTDC are given in Table 1.

Case4: Same to Case3 but both maximum and minimum power flow limits of the DC lines connecting DC bus 3 and 4 are taken to be 0. This case is for the comparison of the meshed MTDC system with the point-to-point HVDC system.

Case5: Same to Case3 but wind power curtailment is not allowed. This case is used to study the impacts of wind power curtailment when using the proposed method.

TABLE 1. MTDC parameters of Case 3.

	VSC				
	Min	Max		Min	Max
U_{c1}	0.9	1.1	U_{c3}	0.9	1.1
U_{dc1}	0.9	1.1	U_{dc3}	0.9	1.1
P_{s1}^{Ref}	-2.0	2.0	P_{s3}^{Ref}	-0.5	0
U_{c2}	0.9	1.1	U_{c4}	0.9	1.1
U_{dc2}	0.9	1.1	U_{dc4}	0.9	1.1
P_{s2}^{Ref}	-2.0	2.0	P_{s4}^{Ref}	-0.5	0

The Grid Code is considered in all the above cases. The SCUC results are presented in Table 2-Table 3 and FIGURE. 6, from which it can be seen that

(1) Case1 and Case2 gives exactly same results. This verifies that the proposed SCUC method for the meshed MTDC/AC system is correct.
(2) The SCUC method proposed in this paper can be conveniently applied to investigate the impact of HVDC system on the UC problem.
(3) The UC cost with the wind farms being connected by the MTDC network (Case3) is less than that with the wind farms being connected by the point-to-point HVDC system. This is because the control flexibility of the MTDC system enables it to coordinate the injected power flow between two grid-connected points of wind power (AC bus3 and bus7)
(4) In case5, during periods of strong wind in both wind farms, generated power cannot be fully delivered though two lines (DC Line 1 and Line 3). Therefore, wind curtailment should be considered in the SCUC for the meshed MTDC/AC systems to ensure the secure of the entire system.

B. DC VOLTAGE DROOP CONTROL

In the test, terminals 3 and 4 are set as constant power control with setting hourly P_s^{Ref} as the corresponding forecasted wind power and other terminal terminals adopt DC droop control strategies. The specified values of DC voltage reference U_{dc}^0 and the slopes R can be obtained by applying the proposed SCUC scheme for the optimal operation of the entire system. To study the impact of these parameters on SCUC problem, the following cases are considered:

Case1: The DC voltage references of U_{dc1}^0 and U_{dc2}^0 are fixed at 1.0 pu. The limits of the slops for converters 1 and 2 are $-15 < R_1 < 15$ and $-15 < R_1 < 15$, respectively.

Case2: The slop constraints are set as same as those for Case1. But the limits of DC voltage references are set as $0.9 \le U_{dc1}^0 \le 1.1$ and $0.9 \le U_{dc2}^0 \le 1.1$.

The Grid Code is considered in both cases. The test results are presents in Table 4. It is found that in both cases the optimal UC cost is achieved. This shows the feasibility and effectiveness of the proposed SCUC scheme for the meshed MTDC/AC system when the DC drop control is used.

TABLE 2. Results of SCUC for different cases.

	Case1	Case2	Case3	Case4	Case5
Objective (10^4 \$)	7.213	7.213	4.344	4.550	Unconverged

TABLE 3. Wind curtailment for Case 3 and Case 4.

	Case3	Case4
Curtailment (MWh)	168.56	292.394
Occurrence (h)	1, 2, 4, 5, 10, 16	1, 2, 4, 5, 8, 9 10, 12, 13, 14, 16, 19, 20, 21, 23

TABLE 4. SCUC results for voltage drop control.

	Case1	Case2
Wind curtailment (MWh)	168.56	168.56
Unit commitment cost (10^4 \$)	4.344	4.344

TABLE 5. SCUC results for voltage drop control.

	Case1	Case2	Case3	Case4
Wind curtailment (MWh)	168.56	155.1`	139.7	153.9
UC cost (104 \$)	4.344	5.446	4.293	5.460

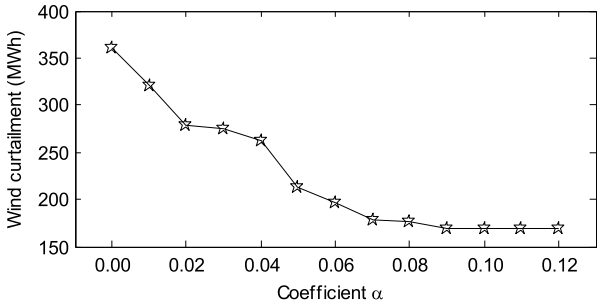

FIGURE 7. Wind curtailment as affected by coefficient α.

C. EFFECTS OF GRID CODE ON THE SCUC

In the study above, the coefficient ruled by the Grid Code in the UK is applied with $\alpha = 0.3287$. However, α may be different in other countries which will influence the SCUC

TABLE 6. Generation data.

Unit No.	Bus	Cost function coefficients a($/MW^2)	b($/MW)	c ($)	Ramp rate MW/h	Pmin MW	Pmax MW	Qmin Mvar	Qmax Mvar	Min On/Off (h)	Start cost $
1	1	0.01	8	80	150	50	150	-100	100	2	100
2	2	0.01	12	120	50	20	50	-50	50	2	100
3	3	0.01	14	140	80	35	80	-60	60	2	50
4	6	0.01	15	150	45	20	45	-40	40	2	40
5	8	0.01	30	300	55	25	55	-30	30	2	10

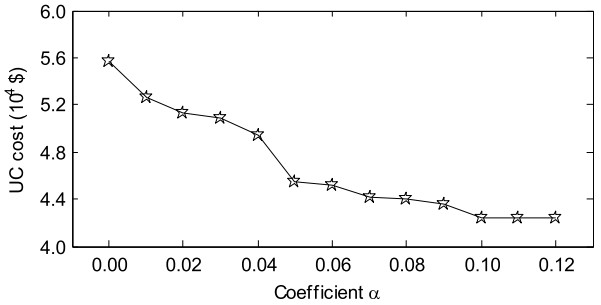

FIGURE 8. UC cost as affected by coefficient α.

results. It can be seen from FIGURE. and FIGURE. that both wind curtailment and the UC cost decrease with the increasing of coefficient α. Hence the Grid Code plays an important role in the SCUC problem for the meshed MTDC/AC systems with wind generation and should be considered in the SCUC scheme.

Coefficient α is the coefficient corresponds to the power factor 0.95. Smaller value of α means tighter constraints of power factor, which can be seen from limit of (15). Therefore, smaller value of α will lead to more wind curtailment.

D. EFFECTS OF MTDC/AC SYSTEM CONFIGURATION ON THE SCUC

Change of connecting locations of the MTDC grid to the AC system and the DC network configuration can affect the SCUC results. Following four cases are designed to compare the effect of the change.

Case1: The meshed VSC-MTDC/AC system is as same as that given in FIGURE. with AC bus 3 and 7 being the connecting locations of the MTDC network to the AC system.

Case2: The connecting locations are changed to AC bus 3 and 4, which are connected with the heaviest power loads.

Case3: Same as Case1. But the DC line connecting DC bus 3 and 4 is removed and DC bus 1 and 2 are connected with a new DC line.

Case4: Same as Case3. But the connecting location of the MTDC network to the AC system are changed to AC bus 3 and 4.

Case1 provides base case for comparison. Case2, Case3 and Case 4 are for the examination of the effect of various factors on the SCUC solution. It can be seen from Table 5 that the UC cost and the required wind curtailment for the meshed VSC-MTDC/AC system change with the change of connecting locations and the configuration of the DC network.

TABLE 7. Bus data [22].

Bus No.	Voltage Min	Voltage Max	Bus No	Voltage Min	Voltage Max
1	1.04	1.07	8	1.02	1.10
2	1.03	1.05	9	1.00	1.03
3	1.00	1.02	10	1.00	1.05
4	1.00	1.03	11	0.98	1.05
5	1.00	1.04	12	1.04	1.07
6	1.05	1.10	13	1.01	1.07
7	1.01	1.05	14	0.98	1.07

TABLE 8. Hourly load distribution.

Hour	MW	MVar	Hour	MW	Mvar
1	181.30	51.45	13	207.20	58.80
2	170.94	48.51	14	196.84	55.86
3	150.22	42.63	15	227.92	64.68
4	143.60	29.40	16	233.10	66.15
5	139.50	36.75	17	220.15	62.48
6	155.40	44.10	18	230.51	65.42
7	181.30	51.45	19	243.46	69.09
8	202.02	57.33	20	253.82	72.03
9	212.38	60.27	21	259.00	73.50
10	227.92	66.68	22	233.10	66.15
11	230.51	65.42	23	225.33	63.95
12	217.56	61.74	24	212.38	60.27

TABLE 9. AC branch data.

Bus	From	To	R(pu)	X(pu)	b(pu)	Flow limit (MW)
1	1	2	0.0194	0.0592	0.0264	50
2	2	3	0.0470	0.1980	0.0219	60
3	2	4	0.0581	0.1763	0.0187	60
4	2	5	0.0570	0.1739	0.0170	60
5	3	4	0.0670	0.1710	0.0173	60
6	4	5	0.0134	0.0421	0.0064	40
7	4	7	0.0000	0.2091	0.0000	65
8	4	9	0.0000	0.5562	0.0000	40
9	5	6	0.0000	0.2520	0.0000	65
10	6	11	0.0950	0.1989	0.0000	50
11	6	12	0.1229	0.1588	0.0000	50
12	6	13	0.0662	0.1303	0.0000	50
13	7	8	0.0000	0.1762	0.0000	50
14	7	9	0.0000	0.1100	0.0000	30
15	9	10	0.0318	0.0845	0.0000	50
16	9	14	0.1271	0.2704	0.0000	50
17	10	11	0.0821	0.1921	0.0000	50
18	12	13	0.2209	0.1999	0.0000	50
19	13	14	0.1709	0.3480	0.0000	50
20	1	5	0.0540	0.2230	0.0246	65

FIGURE.9 gives the UC cost result with the change of the power capacity of the line connecting DC bus 3 and 4 in Case1. The UC cost of the whole system decreases with the increase of the power capacity of the DC line. This is because the MTDC system coordinates the injected power into AC bus 3 and 4 through this DC line. Higher capacity this line

TABLE 10. Distribution factors of loads at different buses.

Bus No.	MW factor	Mvar factor	Bus No.	MW factor	Mvar factor
1	0.0000	0.0000	8	0.0000	0.0000
2	0.0838	0.1728	9	0.1139	0.2259
3	0.3637	0.2585	10	0.0347	0.0789
4	0.1846	-0.0531	11	0.0135	0.0245
5	0.0293	0.0218	12	0.0236	0.0218
6	0.0432	0.1020	13	0.0521	0.0789
7	0.0000	0.0000	14	0.0575	0.0680

TABLE 11. DC transmission line data.

Line No.	From DC bus	To DC bus	R(pu)	Flow Limit (pu)
1	1	3	0.05	0.5
2	3	4	0.04	0.5
3	2	4	0.06	0.5

TABLE 12. Converter parameters.

VSC parameters (pu)			
$R_{tr}=0.0015$	$X_{tr}=0.1121$	$R_c=0.0001$	$X_c=0.0015$
$B_f=0.0887$	$I_{c\max}=1.0526$	$U_{dc\max}=1.2$	$U_{dc\min}=0.8$
VSC loss parameters (pu)			
$a=0.0053$	$b=0.0037$	$c=0.0018$	

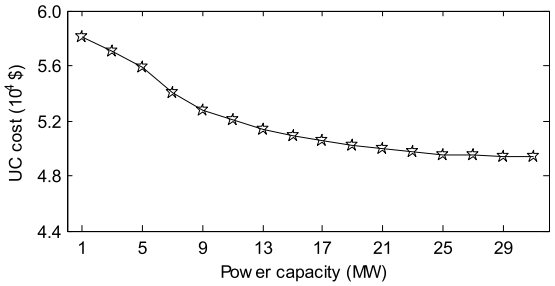

FIGURE 9. UC cost with different power capacity of DC line.

is, more flexibility the MTDC system can have to control the power flow to allocate the available wind power between two connecting locations.

In practice, the selection of connecting locations, the MTDC network configuration and the DC line capacity is determined by many factors, rather than just the operational cost. However, the proposed SCUC model can be used to examine the aspect of operational cost of whole AC/DC system.

V. CONCLUSION

In this paper, a SCUC approach for the meshed VSC-MTDC/AC systems with wind power is presented which could be utilized by the dispatch center to schedule the power generation and wind power economically. The formulated SCUC scheme takes the different control strategies of VSCs and the Grid Code of wind farm interconnection into full consideration. The tests showed the effectiveness of the proposed approach. The proposed scheme can be also used for the selection of connection location of MTDC network of AC grid, the optimization of DC line power capacity, as well as the chosen of the DC network structure.

APPENDIX A
VSC-MTDC/AC JACOBIAN MATRICES

The structure of Jacobian matrix for equality constraints:

$$J=\begin{matrix}\text{AC}&\text{DC}\\ \end{matrix}\begin{bmatrix}J_A & J_B\\ J_C & J_D\end{bmatrix}\begin{matrix}\text{AC}\\ \text{DC}\end{matrix}$$

where $\mathbf{J_A}$ is the Jacobian matrix for AC system, which is provided in [27].

$\mathbf{J_B}=$

	$\boldsymbol{\theta}_f$	$\boldsymbol{\theta}_c$	$\mathbf{U}_f$	$\mathbf{U}_c$	$\mathbf{U}_{dc}$	$\mathbf{Q}_s^{Ref}$	$\mathbf{U}_s^{Ref}$	$\mathbf{R}$
Eq. (1)	$\frac{\partial \text{Eq.(1)}}{\partial \boldsymbol{\theta}_f}$	**0**	$\frac{\partial \text{Eq.(1)}}{\partial \mathbf{U}_f}$	**0**	**0**	**0**	**0**	**0**
Eq. (2)	$\frac{\partial \text{Eq.(2)}}{\partial \boldsymbol{\theta}_f}$	**0**	$\frac{\partial \text{Eq.(2)}}{\partial \mathbf{U}_f}$	**0**	**0**	**0**	**0**	**0**

$\mathbf{J_C}=$

	$\boldsymbol{\theta}$	$\mathbf{U}$	$\mathbf{P_G}$	$\mathbf{Q_G}$
Eq. (7)	$\frac{\partial \text{Eq.(7)}}{\partial \boldsymbol{\theta}}$	$\frac{\partial \text{Eq.(7)}}{\partial \mathbf{U}}$	**0**	**0**
Eq. (8)	$\frac{\partial \text{Eq.(8)}}{\partial \boldsymbol{\theta}}$	$\frac{\partial \text{Eq.(8)}}{\partial \boldsymbol{\theta}}$	**0**	**0**

APPENDIX B
HYBRID VSC-MTDC/AC SYSTEM DATA

See Tables 6–12.

APPENDIX C
WIND DATA (MW)

Hour	WF1	WF2	Hour	WF1	WF2
1	55	65	13	43	56
2	60	66	14	40	54
3	45	29	15	35	11
4	26	38	16	60	6
5	13	12	17	26	15
6	34	14	18	56	21
7	19	27	19	44	45
8	55	45	20	26	15
9	43	17	21	45	34
10	38	55	22	12	31
11	34	23	23	43	55
12	55	45	24	10	24

APPENDIX D
BASE QUANTITIES

Grid frequency 50 Hz
Power 100 MW

REFERENCES

[1] Y. Liu, L. Xiao, H. Wang, S. Dai, and Z. Qi, "Analysis on the hourly spatiotemporal complementarities between China's solar and wind energy resources spreading in a wide area," *Sci. China Technol. Sci.*, vol. 56, no. 3, pp. 683–692, Mar. 2013.

[2] N. Flourentzou, V. G. Agelidis, and G. D. Demetriades, "VSC-based HVDC power transmission systems: An overview," *IEEE Trans. Power Electron.*, vol. 24, no. 3, pp. 592–602, Mar. 2009.

[3] O. Gomis-Bellmunt, J. Liang, J. Ekanayake, R. King, and N. Jenkins, "Topologies of multiterminal HVDC-VSC transmission for large offshore wind farms," *Electr. Power Syst. Res.*, vol. 81, no. 2, pp. 271–281, 2011.
[4] T. Samus, B. Lang, and H. Rohn, "Assessing the natural resource use and the resource efficiency potential of the Desertec concept," *Sol. Energy*, vol. 87, pp. 176–183, Jan. 2013.
[5] J. De Decker and A. Woyte, "Review of the various proposals for the European offshore grid," *Renew. Energy*, vol. 49, pp. 58–62, Jan. 2013.
[6] J. G. Chen, C. B. Yu, T. T. Sun, and K. J. Ou, "Characteristics analysis and simulation testing on modular multilevel converter VSC-HVDC based on RTDS," *Appl. Mech. Mater.*, vols. 397–400, pp. 1794–1799, Sep. 2013.
[7] H. Ambriz-Pérez, E. Acha, and C. R. Fuerte-Esquivel, "High voltage direct current modelling in optimal power flows," *Int. J. Electr. Power Energy Syst.*, vol. 30, no. 3, pp. 157–168, Mar. 2008.
[8] N. P. Padhy, "Unit commitment—A bibliographical survey," *IEEE Trans. Power Syst.*, vol. 19, no. 2, pp. 1196–1205, May 2004.
[9] V. Sarkar and S. A. Khaparde, "Implementation of LMP-FTR mechanism in an AC-DC system," *IEEE Trans. Power Syst.*, vol. 23, no. 2, pp. 737–746, May 2008.
[10] J. Wang, M. Shahidehpour, and Z. Li, "Security-constrained unit commitment with volatile wind power generation," *IEEE Trans. Power Syst.*, vol. 23, no. 3, pp. 1319–1327, Aug. 2008.
[11] Y. Fu, C. Wang, W. Tian, and M. Shahidehpour, "Integration of large-scale offshore wind energy via VSC-HVDC in day-ahead scheduling," *IEEE Trans. Sustain. Energy*, vol. 7, no. 2, pp. 535–545, Apr. 2016.
[12] A. Lotfjou, M. Shahidehpour, Y. Fu, and Z. Li, "Security-constrained unit commitment with AC/DC transmission systems," *IEEE Trans. Power Syst.*, vol. 25, no. 1, pp. 531–542, Feb. 2010.
[13] B. Zhou, X. Ai, J. Fang, J. Wen, and J. Yang, "Mixed-integer second-order cone programming taking appropriate approximation for the unit commitment in hybrid AC–DC grid," *J. Eng.*, vol. 2017, no. 13, pp. 1462–1467, Jan. 2017.
[14] M. Baradar, M. R. Hesamzadeh, and M. Ghandhari, "Second-order cone programming for optimal power flow in VSC-type AC-DC grids," *IEEE Trans. Power Syst.*, vol. 28, no. 4, pp. 4282–4291, Nov. 2013.
[15] L. Jun, J. Tianjun, O. Gomis-Bellmunt, J. Ekanayake, and N. Jenkins, "Operation and control of multiterminal HVDC transmission for offshore wind farms," *IEEE Trans. Power Del.*, vol. 26, no. 4, pp. 2596–2604, Oct. 2011.
[16] T. M. Haileselassie and K. Uhlen, "Impact of DC line voltage drops on power flow of MTDC using droop control," *IEEE Trans. Power Syst.*, vol. 27, no. 3, pp. 1441–1449, Aug. 2012.
[17] J. Beerten, S. Cole, and R. Belmans, "Generalized steady-state VSC MTDC model for sequential AC/DC power flow algorithms," *IEEE Trans. Power Syst.*, vol. 27, no. 2, pp. 821–829, May 2012.
[18] X.-P. Zhang, "Multiterminal voltage-sourced converter-based HVDC models for power flow analysis," *IEEE Trans. Power Syst.*, vol. 19, no. 4, pp. 1877–1884, Nov. 2004.
[19] L. Xu, L. Yao, and C. Sasse, "Grid integration of large DFIG-based wind farms using VSC transmission," *IEEE Trans. Power Syst.*, vol. 22, no. 3, pp. 976–984, Aug. 2007.
[20] S. Engelhardt, I. Erlich, J. Kretschmann, F. Shewarega, and C. Feltes, "Reactive power capability of wind turbines based on doubly fed induction generators," *IEEE Trans. Energy Convers.*, vol. 26, no. 1, pp. 364–372, Mar. 2011.
[21] Y. Fu, M. Shahidehpour, and Z. Li, "Security-constrained unit commitment with AC constraints," *IEEE Trans. Power Syst.*, vol. 20, no. 2, pp. 1001–1013, May 2005.
[22] G. Strbac, A. Shakoor, M. Black, D. Pudjianto, and T. Bopp, "Impact of wind generation on the operation and development of the UK electricity systems," *Electr. Power Syst. Res.*, vol. 77, no. 9, pp. 1214–1227, 2007.
[23] Y. V. Makarov, C. Loutan, J. Ma, and P. D. Mello, "Operational impacts of wind generation on California power systems," *IEEE Trans. Power Syst.*, vol. 24, no. 2, pp. 1039–1050, May 2009.
[24] M. Albadi and E. El-Saadany, "Comparative study on impacts of wind profiles on thermal units scheduling costs," *IET Renew. Power Gener.*, vol. 5, no. 1, pp. 26–35, Nov. 2011.
[25] B. A. McCarl, *McCarl GAMS User Guide Version 22.0*, GAMS Development Corporation, Fairfax, VA, USA, 2006.
[26] J. Cao, W. Du, H. F. Wang, and S. Q. Bu, "Minimization of transmission loss in meshed AC/DC grids with VSC-MTDC networks," *IEEE Trans. Power Syst.*, vol. 28, no. 3, pp. 3047–3055, Aug. 2013.
[27] R. D. Zimmerman, C. E. Murillo-Sanchez, and R. J. Thomas, "MATPOWER: Steady-state operations, planning, and analysis tools for power systems research and education," *IEEE Trans. Power Syst.*, vol. 26, no. 1, pp. 12–19, Feb. 2011.

ZHUOYU JIANG is working with Three Gorges Power Corporation Ltd. His research interests include the economic analysis and the operation of the micro-grid.

YI LIU received the B.S. degree from the School of Electrical Engineering, Tianjin University, China, and the Ph.D. degree from the Institution of Electrical Engineering, Chinese Academy of Sciences.

His research interests include the economic and stability analysis of power systems operation, including renewable power and multi-terminal DC power systems.

ZHE KANG is working with Three Gorges Power Corporation Ltd. His research interests include the economic analysis and the operation of PV generation and operation of the micro-grid.

TAO HAN is working with Three Gorges Power Corporation Ltd. His research interests include the economic analysis and the operation of PV generation and operation of the micro-grid.

JING ZHOU is working with Three Gorges Power Corporation Ltd. His research interests include the economic analysis and the operation of PV generation and operation of the micro-grid.